

Vapor–Liquid Equilibria for Binary Mixtures of CO₂ with 2-Methyl-2-propanol, 2-Methyl-2-butanol, Octanoic Acid, and Decanoic Acid at Temperatures from 313.15 K to 353.15 K and Pressures from 3 MPa to 24 MPa

Joo-Hyung Heo, Hun Yong Shin, Ji-Ung Park, Seung Nam Joung, Sun Young Kim, and Ki-Pung Yoo*

Laboratory of Thermodynamics & Supercritical Fluid Engineering, Department of Chemical Engineering, Sogang University, C.P.O. Box 1142, Seoul, Korea

Phase behaviors of mixtures of CO₂ with 2-methyl-2-propanol, 2-methyl-2-butanol, octanoic acid, and decanoic acid were measured with a variable-volume view-cell apparatus from 313.15 K to 353.15 K and from 3 MPa to 24 MPa. The results were correlated by the multifluid–nonrandom lattice fluid (MF–NLF) equation of state.

Introduction

Enzymatic synthesis of biologically active materials using a nonconventional medium such as a supercritical fluid has received much attention in recent years.^{1,2} Among various supercritical fluids, supercritical carbon dioxide (SC-CO₂) has gained significant attention as an enzymatic reaction medium. The use of SC-CO₂ has several advantages such as high reaction rate, high mass transfer, nontoxicity, nonflammability, and low cost. Enzymes, especially lipase, exhibit a stable activity in SC-CO₂.³ The most important aspect of supercritical fluids is that a slight change in pressure can readily vary the solubility of the substrate and product in a supercritical fluid medium. To design such a high-pressure reaction system, knowledge of the solubility and phase behavior for the substances (reactant, product, cosolvent, etc.) and their mixture in SC-CO₂ is important to establish suitable conditions for the enzymatic reaction within a supercritical medium.

In this study, a lipase-catalyzed acylation of sugar and a medium-chain fatty acid in SC-CO₂ by doping a cosolvent is chosen as the model system for examination. For determining the phase behavior of this system, single phases for binary mixtures of reactant (octanoic acid and decanoic acid) and cosolvent (2-methyl-2-propanol and 2-methyl-2-butanol) with SC-CO₂ were measured in a variable-volume view-cell apparatus over a wide range of temperatures (313.15 K to 353.15 K) and pressures (3 MPa to 24 MPa). Furthermore, to provide phase equilibrium information for high-pressure process design purposes the measured vapor–liquid equilibrium (VLE) behavior data of binary systems were correlated by a lattice-theory-based equation of state (MF–NLF EOS). These results can give valuable information for rational design and operation of the supercritical-phase enzymatic reaction.

Experimental Section

Apparatus. A schematic diagram of a variable-volume view cell is shown in Figure 1. The internal volume of the cell was 33.0 cm³. This apparatus was designed to operate up to 35 MPa and up to 473.15 K. The valves were from

* To whom correspondence should be addressed. Fax: 82-2-3272-0331. E-mail: kpyoo@ccs.sogang.ac.kr.

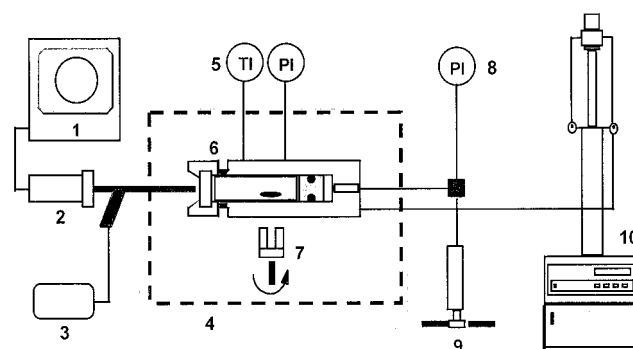


Figure 1. Schematic diagram of the high-pressure variable-volume view cell: 1, monitor; 2, CCD camera; 3, halogen light source; 4, air oven; 5, temperature indicator; 6, variable volume view cell; 7, magnetic stirrer; 8, pressure indicator; 9, pressure generator; 10, syringe pump.

Autoclave Inc. (Erie, PA), and the syringe pump (ISCO 260DM, Lincoln, NE) was equipped to charge CO₂ with a volume uncertainty of 2%. Materials were charged into the cell using a Fisher Hamilton syringe (Pittsburgh, PA). The pressure in the cell was generated via pressurization of pistons containing silicon oil by a pressure generator (model no. 550.0202.1, NOVA, Swiss). The equilibrium pressure in the cell was measured by a differential pressure gauge (ISI 0163-5, OCB, Winchester, MA), which was confirmed by a Heise pressure gauge (HEISE MM-43776, CT) within the uncertainty range of ± 0.05 MPa. The temperature in the cell was maintained by a PID regulator (Hanyoung Co., Seoul, Korea) in an air bath (Jeio Tech. FO-600M, Seoul, Korea) within ± 1.0 K. The error range of measured temperatures was within ± 0.1 K, which was confirmed by a standard high-precision thermometer (Witeg, Germany). The reliability of material feeding and the reading accuracy of temperature and pressure was confirmed by comparison with the published data of a methanol + CO₂ system.⁴ A sapphire window was attached at the front end of the cell, and phase equilibrium behavior was observed by a charge-coupled device with a halogen light source, a camera (Toshiba IK-C41MF, Japan), and the real time frame Grabber (Data Translation Co., MASH Series DT3155,

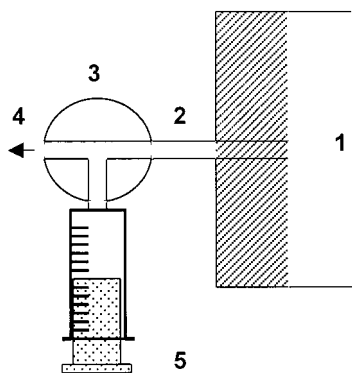


Figure 2. Schematic diagram of the syringe injection for sample loading into the equilibrium cell: 1, equilibrium cell; 2, three-way valve; 3, injection port; 4, waste port; 5, syringe.

MA). A magnetic stirrer was used for mixing the fluid in the cell.

Experiment. High-purity grade (99+%) octanoic acid, decanoic acid, 2-methyl-2-propanol, and 2-methyl-2-butanol from Aldrich Co. (Milwaukee, WI) was used. CO₂ (>99.9%) was purchased from Seoul Gas Co. (Seoul, Korea). For each run, the entire line was evacuated by a vacuum pump. While keeping the cell evacuated, a known volume of the alcohol or fatty acid, which was degassed under reduced pressure, was charged into the cell with a syringe via the three-way valve. As shown in Figure 2, air existing between the three-way valve and the syringe was completely removed by discharging some portion of sample from the syringe by opening the waste valve. In the next step, the remaining portion of sample in the syringe was naturally fed into the evacuated equilibrium cell by cautiously closing the waste valve and opening the injection valve. The amount of sample fed into the cell was determined by reading the difference of the calibrated void volume of the three-way valve and the reduced volume of the syringe. A known volume of liquid CO₂ at 313.15 K and 20 MPa was charged into the cell from the ISCO syringe pump. While maintaining an isothermal condition of the cell, the mixture of the sample with CO₂ was pressurized to a higher pressure until the mixture was a single phase. Phase behavior in the cell was observed with the on-line computer monitor. After it was confirmed that the fluid mixture was still one phase, the pressure in the cell was slowly lowered using the pressure generator. Then, the transition pressure (the pressure at which the two-phase to one-phase transition takes place) was measured. For each mixture, the measurement of the pressure when the second phase appeared was repeated three times.

Thermodynamic Modeling of VLE Data

To model the phase behavior of pure fluids and mixtures, an equation of state (EOS) developed recently by the present authors was adopted. The MF-NLF EOS originates from the nonrandom lattice-hole theory.^{5,6} The final expression for the EOS is written for a general mixture as

$$P = \frac{1}{\beta V_H} \left\{ \frac{z}{2} \ln \left[1 + \left(\frac{q_M}{r_M} - 1 \right) \rho \right] - \ln(1 - \rho) + \frac{z}{2} \sum_{i=1}^c \theta_i \left(\frac{\tau_{0i}}{\sum_{k=0}^c \theta_k \tau_{ki}} - 1 \right) \right\} \quad (1)$$

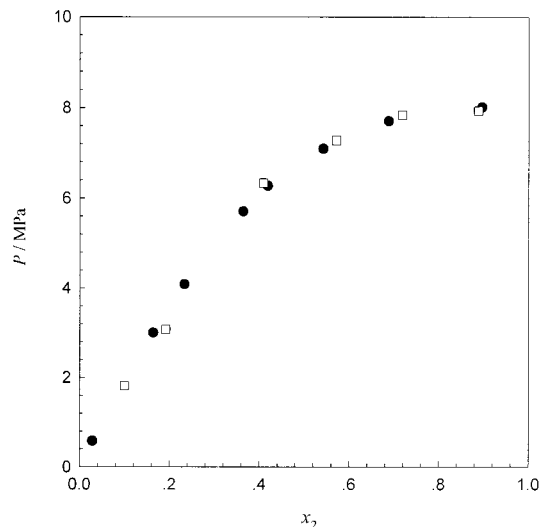


Figure 3. Phase behavior of methanol (1) + CO₂ (2) at 313.15 K: □, data obtained in this work; ●, data reported by Ohgaki et al. (ref 6).

$$\tau_{ji} = \exp\{\beta(\epsilon_{ji} - \epsilon_{ij})\} \quad (2)$$

where P is the pressure, β is the Boltzmann factor, V_H is the unit lattice site volume, z is the coordination number, q_M is the average surface area parameter for mixture, r_M is the average segment number, ρ is the density, θ_i is the surface area fraction of component i , τ_{ji} is the nonrandomness factor, and x_i is the mole fraction of species i . We set the coordination number (z) as 10 and the unit lattice cell volume (V_H) as 9.75 cm³/mol⁻¹. If we set the subscripts $i = 1$ and $j = 0$ in eq 1, the EOS is reduced to an expression for pure fluid. ϵ_{ji} is the absolute value of the interaction energy between segments of species j and i . ϵ_{ji} between holes and molecular species is zero.

The two molecular parameters in the EOS for a pure fluid, R_1 and ϵ_{11} , were determined from the estimated molar volumes and vapor pressures of the pure components, and they were fitted by the following empirical expressions:

$$\epsilon_{11}/k = E_a + E_b(T - T_0) + E_c(T \ln T/T_0 + T - T_0) \quad (3)$$

$$R_1 = R_a + R_b(T - T_0) + R_c(T \ln T/T_0 + T - T_0) \quad (4)$$

where k is the Boltzmann constant, the reference temperature, T_0 , is 298.15 K, and E_a , E_b , E_c , R_a , R_b , and R_c are the fitting parameters. We have one binary energy parameter λ_{12} for a binary component 1 and 2, which is defined by

$$\epsilon_{12} = (\epsilon_{11}\epsilon_{22})^{1/2}(1 - \lambda_{12}) \quad (5)$$

λ_{12} is determined by data fitting and may be temperature dependent. The estimated values for the coefficients in eqs 3 and 4 are summarized in Tables 5 and 6 for the binary mixtures. For a binary mixture, the cross interaction energy ϵ_{12} in eq 5 is empirically fit to the experimental data for the binary mixtures, and these values are summarized in Table 7.

Single-Phase Limit for Binary Mixtures

To check the reliability of the apparatus, transition pressures were measured for methanol + CO₂ at 313.15 K over the entire range of concentrations of methanol and the results were compared with existing reliable data⁴ in Figure 3. After checking the reliability, the phase behaviors

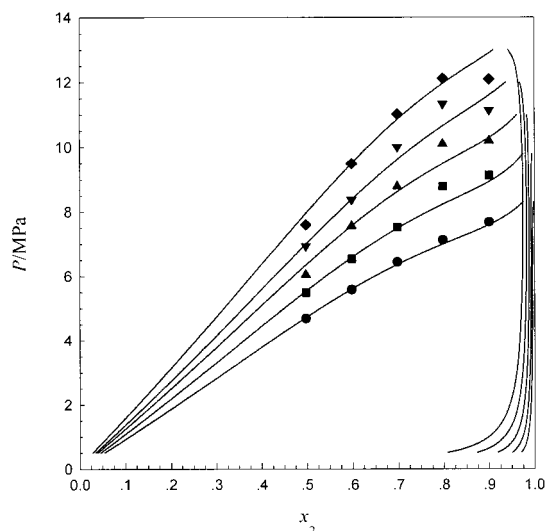


Figure 4. Locus of transition pressures vs mole fraction of CO₂ in 2-methyl-2-propanol (1) + CO₂ (2) system: ●, 313.15 K; ■, 323.15 K; ▲, 333.15 K; ▼, 343.15 K; ◆, 353.15 K; solid line, MF-NLF EOS ($\lambda_{12} = 0.09558$).

Table 1. P - T - x Surface for Single-Phase Limit of 2-Methyl-2-propanol (1) + CO₂ (2) System

x_1	0.0999	0.2020	0.3021	0.4018	0.5025
T/K	P/MPa				
313.15	7.67	7.30	6.43	5.57	4.67
323.15	9.12	8.78	7.52	6.54	5.49
333.15	10.18	10.10	8.78	7.55	6.04
343.15	11.13	11.33	9.99	8.37	6.94
353.15	11.69	12.12	11.02	9.49	7.59

Table 2. P - T - x Surface for Single-Phase Limit of 2-Methyl-2-butanol (1) + CO₂ (2) System

x_1	0.0998	0.1999	0.2986	0.4003	0.4959	0.5920
T/K	P/MPa					
313.15	7.62	7.08	6.62	5.84	4.44	3.62
323.15	9.28	8.32	7.57	6.78	5.18	4.20
333.15	10.59	9.59	8.59	7.74	5.75	4.70
343.15	11.81	11.10	9.74	8.58	6.47	5.19
353.15	12.95	12.26	10.74	9.46	7.06	5.81

Table 3. P - T - x Surface for Single-Phase Limit of Octanoic Acid (1) + CO₂ (2) System

x_1	0.0924	0.153	0.202	0.296	0.345	0.398	0.454
T/K	P/MPa						
313.15	10.40	9.99	9.23	8.13	7.48	6.89	5.89
323.15	13.23	12.71	11.09	9.06	8.42	7.88	6.83
333.15	15.87	15.28	13.49	10.46	9.44	8.45	7.47
343.15	18.41	17.92	16.08	12.29	10.66	9.73	8.49
353.15	20.59	20.15	18.30	14.51	12.49	11.05	9.52

Table 4. P - T - x Surface for Single-Phase Limit of Decanoic Acid (1) + CO₂ (2) System

x_1	0.102	0.178	0.306	0.398	0.502	0.607
T/K	P/MPa					
313.15	13.79	10.30	7.54	5.14	3.97	2.21
323.15	16.76	13.16	8.48	6.61	4.69	2.85
333.15	19.39	15.80	9.32	7.77	5.71	3.81
343.15	21.59	18.22	10.75	8.77	6.52	4.45
353.15	23.77	20.43	11.91	10.09	7.73	5.07

of 2-methyl-2-propanol + CO₂, 2-methyl-2-butanol + CO₂, octanoic acid + CO₂, and decanoic acid + CO₂ were

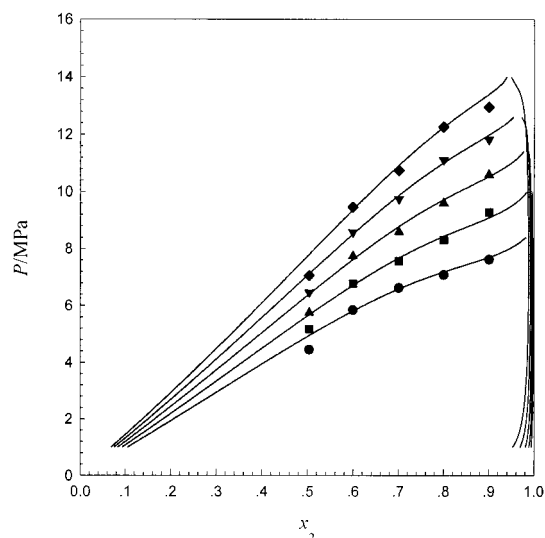


Figure 5. Locus of transition pressures vs mole fraction of CO₂ in 2-methyl-2-butanol (1) + CO₂ (2) system: ●, 313.15 K; ■, 323.15 K; ▲, 333.15 K; ▼, 343.15 K; ◆, 353.15 K; solid line, MF-NLF EOS ($\lambda_{12} = 0.06802$).

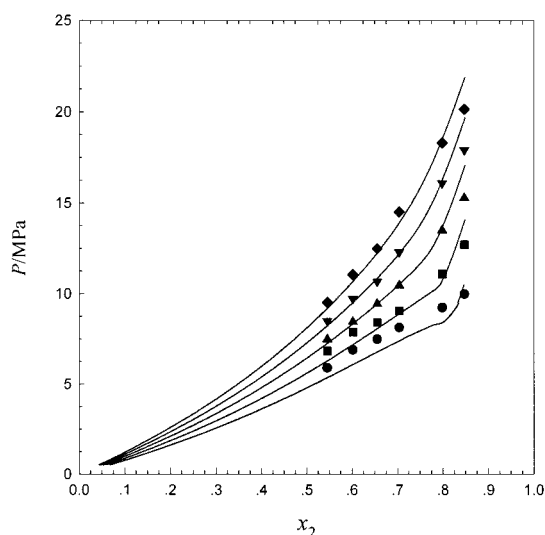


Figure 6. Locus of transition pressures vs mole fraction of CO₂ in octanoic acid (1) + CO₂ (2) system: ●, 313.15 K; ■, 323.15 K; ▲, 333.15 K; ▼, 343.15 K; ◆, 353.15 K; solid line, MF-NLF EOS ($\lambda_{12} = 0.03757$).

Table 5. Coefficients of MF-NLF Energy Parameter Correlation Given by Equation 3

system	E_a	E_b	E_c
carbon dioxide	85.9130	-0.10298	-0.03656
2-methyl-2-propanol	120.6273	-0.10762	-0.2237
2-methyl-2-butanol	110.0519	-0.10337	-0.2627
octanoic acid	143.8796	-0.09471	-0.1253
decanoic acid	148.4838	-0.014559	-0.2396

determined. Phase behavior data for the *tert*-alcohol + CO₂ systems were measured at various conditions (0.0999 to 0.5025 mole fraction of 2-methyl-2-propanol and 0.0998 to 0.592 mole fraction of 2-methyl-2-butanol at 313.15 K to 353.15 K), and these results were summarized in Tables 1 and 2. The results for medium-chain fatty acid + CO₂ systems at various equilibrium conditions (0.0924 to 0.454 mole fraction of octanoic acid and 0.102 to 0.607 mole fraction of decanoic acid at 313.15 K to 353.15 K) were summarized in Tables 3 and 4. The standard deviation of the phase transition pressures measured in the present work was within $\pm(0.05$ to $0.20)$ MPa. The data sum-

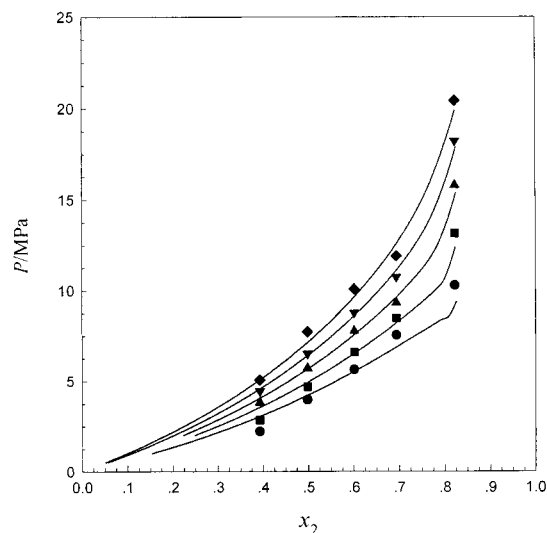


Figure 7. Locus of transition pressures vs mole fraction of CO₂ in decanoic acid (1) + CO₂ (2) system: ●, 313.15 K; ■, 323.15 K; ▲, 333.15 K; ▼, 343.15 K; ◆, 353.15 K; solid line, MF–NLF EOS ($\lambda_{12} = 0.01849$).

Table 6. Coefficients of MF–NLF Size Parameter Correlation Given by Equation 4

system	R_a	R_b	R_c
carbon dioxide	34.2861	0.01428	−0.01304
2-methyl-2-propanol	97.0196	−0.00056	0.03096
2-methyl-2-butanol	101.9399	−0.00778	0.1446
octanoic acid	141.4635	0.05232	0.01669
decanoic acid	171.8382	−0.07351	−0.1319

marized in Tables 1 to 4 and the P – x diagrams were plotted in Figures 4, 5, 6, and 7. The experimental data were correlated using the MF–NLF EOS. On the basis of the EOS parameters for each pure fluid and their mixtures in Tables 5 to 7, experimental VLE results of 2-methyl-2-propanol + CO₂, 2-methyl-2-butanol + CO₂, octanoic acid + CO₂, and decanoic acid + CO₂ were correlated by the EOS. These calculated results were compared with the measured data in Figures 4 to 7. When the experimental

Table 7. Best-Fitted Binary Interaction Energy Parameters

binary system	binary interaction parameter
CO ₂ + 2-methyl-2-propanol	0.095 58
CO ₂ + 2-methyl-2-butanol	0.068 02
CO ₂ + octanoic acid	0.030 93
CO ₂ + decanoic acid	0.018 49

data were fitted by the MF–NLF EOS, there are some correlation inaccuracies in the vicinity of the critical point because of the mean-field approximation nature of the underlying lattice-hole theory.⁵ To date, any EOS model stemming from the classical theory, such as the cubic EOS, experiences the same erroneous aspect in the near-critical region. To overcome this inaccuracy, it is necessary to combine the EOS with the nonclassical scaling theory. However, except in the critical region the EOS fit the data reasonably well.

Literature Cited

- (1) Castillo, E.; Marty, A.; Combes, D.; Condoret, J. S. Polar Substrates for Enzymatic Reactions in Supercritical CO₂: How to Overcome the Solubility Limitation. *Biotechnol. Lett.* **1994**, *16*, 169–174.
- (2) Russell, A. J.; Beckman, E. J.; Chaudhary, A. K. Studying Enzyme Activity in Supercritical Fluids. *CHEMTECH* **1994**, *24*, 33–37.
- (3) Marty, A.; Combes, D.; Condoret, J.-S. Continuous Reaction-Separation Process for Process for Enzymatic Esterification in Supercritical Carbon Dioxide. *Biotechnol. Bioeng.* **1994**, *43*, 497–504.
- (4) Ohgaki, K.; Katayama, T. Isothermal Vapor-Liquid Equilibrium Data for Binary Systems Containing Carbon Dioxide at High Pressures: Methanol-Carbon Dioxide, *n*-Hexane-Carbon Dioxide, and Benzene-Carbon Dioxide Systems. *J. Chem. Eng. Data* **1976**, *21*, 53–55.
- (5) Yoo, K.-P.; Shin, H. Y.; Lee, C. S. Approximate Nonrandom Two-Fluid Lattice Theory. General Derivation and Description of Pure Fluids. *Bull. Korean Chem. Soc.* **1997**, *18*, 965–972.
- (6) Yoo, K.-P.; Shin, H. Y.; Lee, C. S. Approximate Nonrandom Two-Fluid Lattice Hole Theory. General Derivation and Description of Pure Fluid. *Bull. Korean Chem. Soc.* **1997**, *18*, 841–850.

Received for review February 14, 2000. Accepted December 4, 2000. The authors acknowledge the Korea Research Foundation for financial support.

JE0000540